



(Submitted to the APS Division of
Particles and Fields Meeting, Berkeley,
California, August 13-17, 1973)

π^- p INTERACTIONS AT 205 GeV/c: CROSS SECTIONS
AND CHARGED PARTICLE MULTIPLICITY

D. Bogert, R. Hanft, F. R. Huson, D. Ljung,
C. Pascaud, S. Pruss, and W. M. Smart
National Accelerator Laboratory, Batavia, Illinois

and

G. S. Abrams, H. H. Bingham, D. M. Chew, B. Y. Daugéras,
W. B. Fretter, C. E. Friedberg, G. Goldhaber, W. R. Graves,
A. D. Johnson, J. A. Kadyk, L. Stutte, G. H. Trilling,
F. C. Winkelmann, and G. P. Yost
Department of Physics and Lawrence Berkeley Laboratory
University of California, Berkeley, California

August 1973



π^-p INTERACTIONS AT 205 GeV/c: CROSS SECTIONS
AND CHARGED PARTICLE MULTIPLICITY*

D. Bogert, R. Hanft, F. R. Huson, D. Ljung,
C. Pascaud,[†] S. Pruss, and W. M. Smart

National Accelerator Laboratory, Batavia, Illinois 60510

and

G. S. Abrams, H. H. Bingham, D. M. Chew, B. Y. Daugéras,[†]
W. B. Fretter, C. E. Friedberg, G. Goldhaber, W. R. Graves,
A. D. Johnson, J. A. Kadyk, L. Stutte, G. H. Trilling,
F. C. Winkelmann, and G. P. Yost

Department of Physics and Lawrence Berkeley Laboratory
University of California, Berkeley, California 94720

Results are reported based on a study of 3114 π^-p events at 205 GeV/c in the NAL 30" bubble chamber. The measured π^-p total and elastic cross sections are 24.0 ± 0.5 and 3.0 ± 0.3 mb respectively. The elastic differential cross section has a slope of $9.0 \pm 0.7 \text{ GeV}^{-2}$ for $0.03 \leq -t \leq 0.6 \text{ GeV}^2$. The average charged particle multiplicity for the inelastic events is 8.02 ± 0.12 .

This paper presents measurements of the total cross section, elastic cross section, and charged particle multiplicity distribution for 205 GeV/c π^-p interactions in the NAL 30" hydrogen bubble chamber. Both the total and elastic cross sections are found to be consistent with those observed in the 40-60 GeV/c

range.^{1, 2} The multiplicity distribution is similar to that observed in 205 GeV/c pp interactions,³ but the average π^-p multiplicity is somewhat higher.

Beam. An unseparated 205 GeV/c negative particle beam was produced by targeting 303 GeV/c protons from the NAL synchrotron and was transported 1.0 km to the bubble chamber. The beam at the bubble chamber had a momentum spread of $\pm 0.1\%$ and angular divergence of ± 0.25 mrad, a muon contamination of $2.2 \pm 0.3\%$ determined by an absorption measurement, and K^- and \bar{p} proportions of $1.4 \pm 0.2\%$ and $0.16 \pm 0.1\%$, respectively, obtained from differential gas Cerenkov counter measurements.

Scanning and Measurement. The film was scanned in three views with approximately lifesize projection. The accepted events were restricted to a fiducial volume of length 39.3 ± 0.2 cm in the beam direction with an entrance plane 12 cm downstream of the bubble chamber window. A total of 7,700 photographs in which more than 15 tracks crossed the fiducial volume entrance were not used in this analysis. In the remaining 14,285 frames the recorded information included: the number of beam tracks (tracks having a divergence ≤ 2.0 mrad from nominal) entering the fiducial volume; the number of prongs and distance from the primary vertex for all secondary interactions; vees from neutral particle decays or gamma conversions and their distances from the primary interaction; and π^0 decays. The film was scanned in this manner once by physicists and independently a second time by professional scanners. Discrepancies were resolved on a scan table providing 3.5x lifesize images.

Events were measured on film plane digitizers and processed by the standard reconstruction and fitting programs TVGP and SQUAW. Elastic and Total Cross Sections. In the determination of the incident pion flux, the following potential sources of systematic error were considered: (1) beam track scanning efficiency ($99.5 \pm 0.5\%$); (2) muon contamination at the bubble chamber ($2.2 \pm 0.3\%$); (3) K^- and \bar{p} contamination, leading to a negligible net cross section correction ($0.0 \pm 0.2\%$); (4) contamination from forward secondaries of upstream interactions ($0.0 \pm 0.6\%$); (5) electron contamination ($< 0.5\%$). The total pion beam path length after all corrections, was $(3.56 \pm 0.04) \times 10^6$ cm.

From measurement of ranges of muons from π^+ decays at rest, the hydrogen density was determined to be 0.0627 ± 0.0005 gm/cm³.

The scanning efficiency for events having four or more prongs was 99.9% after the double scan. The scanning efficiency for two-prong events, except for those with recoil protons less than 2 cm long, was 99.5%.

Elastic events, which constitute about 2/3 of the two-prong sample, were identified by kinematic fitting. A study of transverse momentum balance indicated that the successful fits contained a 5% contamination from inelastic events for which a correction⁴ was made in determining cross sections. The elastic differential cross section is shown in Fig. 1a. The slope parameter b , determined from fitting $d\sigma/dt$ to the form Ae^{bt} for $0.03 < -t < 0.6$ GeV², is 9.0 ± 0.7 GeV⁻². After a 12% correction⁵ to the two-prong sample to take account of systematic scanning

loss at low t for both elastic and two-prong inelastic events, we find total and elastic cross sections of 24.0 ± 0.5 and 3.0 ± 0.3 mb. It should be noted from Fig. 1a that the elastic differential cross section, extrapolated to $t = 0$ with constant slope b , is consistent with the optical point calculated from our measured total cross section.

Figures 1b and 1c show the momentum dependence of the total and elastic π^-p cross sections. The cross sections are the same, within the errors, at Serpukhov energies (40-60 GeV/c) and 205 GeV/c.

Charged-Particle Multiplicity. The first two columns of Table I give the raw charged-particle multiplicity data found in the scanning process. To obtain an unbiased multiplicity distribution, these data were corrected for the following effects.

(i) Secondary interactions may occur close to the primary vertex and hence be unresolved from the primary interaction. This effect is the primary cause of the odd-prong populations for the raw data given in Table I. (The other source is events with unseen protons. We expected five such diffractive events and found three not counting one-prongs.) To correct for the remaining odd-prong events a comparison was made between the scanned prong distribution from secondary interactions less than 40 mm from the primary interaction and that from secondaries beyond 40 mm where few are missed. This resulted in the assignment of a primary multiplicity of five less than the scanned number of prongs for odd-prong events. This comparison also indicated that a greater number of close secondaries were missed than accounted for by

odd-prong events, and that these secondaries were two-prong events with a slow proton which was also missed. Hence, no correction for these is required

(ii) Electron pairs and vee decays close to the primary vertex can also contribute to the observed prong multiplicities. Again the number of these was determined from a study of the distribution of scanned pairs and vees as a function of associated event multiplicity and as a function of distance between the primary interaction and the scanned pair or vee.

(iii) Dalitz decays, which are included in the prong counts of the raw multiplicity data, were statistically removed on the basis of our observations of resolved electron pairs.

The third and fourth columns of Table I give the corrected multiplicity distributions, errors, and corresponding cross sections.

Some moments of the multiplicity distribution are defined and are given in Table II for this experiment and for 205 GeV/c pp.⁸ The moments for π^-p and pp interactions are similar, however $\langle n_{ch} \rangle$ and $\langle n_{ch}(n_{ch}-1) \rangle$ for π^-p are greater than the corresponding pp values at 205 GeV/c and also at lower energies.⁹ For the same Q (center-of-mass energy minus incident particle masses) this difference is smaller but still nonzero. For π^-p both at Serpukhov energies¹⁰ and at 205 GeV/c, $\langle n_{ch} \rangle/D$ is nearly two. The data expressed in any one of the usual variables $\langle n_{ch} \rangle$, $\langle n_{ch}^- \rangle$ (number of negatives), $\langle n_{ch}^- - 1 \rangle / 2$ and $\langle n_{ch}^- - 2 \rangle / 2$ do not fit a Poisson distribution.

It is a pleasure to acknowledge the effort put forth by the 30-inch bubble chamber staff, the hadron beam group, and the accelerator operations personnel. We wish also to thank the NAL scanning staff and the Berkeley measuring staff.

*Work supported in part by the U.S. Atomic Energy Commission, the National Science Foundation, and the French CNRS.

†On leave of absence from LAL, Orsay, France.

¹S. P. Denisov, et. al., Phys. Lett. 36B, 528 (1971).

²A. P. Bugorsky, et.al., Studying Elastic Scattering of Negative Pions on Protons at Small Angles in Momentum Range 30-55 GeV/c, Paper submitted to XVIth International Conference on High-Energy Physics, Batavia, 1972.

³G. Charlton, et. al., Phys. Rev. Lett. 29, 515 (1972).

⁴In the calculation of transverse momentum imbalance (Δp_t) a momentum of 205 GeV/c was assigned to the outgoing π^- and its π^- direction at the primary vertex was recalculated. The resulting resolution in the component of Δp_t perpendicular to the lens axis, $\Delta p_{t\phi}$, is ± 50 MeV/c. The reaction $\pi^- p \rightarrow \pi^- \pi^0 \pi^0 p$ with all π 's forward is expected to be the main source of the small inelastic background under the elastic peak in $\Delta p_{t\phi}$. (Events with backward π^0 's yield a missing mass to the proton easily distinguishable from the π^- mass and unless G parity exchange processes are unexpectedly large, few events should have 1 or 3 forward π^0 's.) We study this $\pi^- \pi^0 \pi^0 p$ background by dropping 2 π 's from 4-prong events and subjecting these pseudo 2-prong events to the same analysis used for

real 2-prongs. The broad $|\Delta p_{t\phi}|$ distribution from these events agrees in shape and approximate magnitude with that observed in the real 2-prong events outside the elastic peak, ($|\Delta p_{t\phi}| > 250$ MeV/c). Thus we have used the pseudo 2-prong background distribution to subtract an $\sim 5\%$ background under the elastic peak.

⁵This correction was made by extrapolating $d\sigma/dt$ elastic from $|t| = 0.03$ to 0.0 GeV^2 with the same slope b . The inelastic 2-prong events for $t < .03$ GeV^2 were corrected by assuming the same fraction of lost events as for elastics.

⁶K. J. Foley, et. al., Phys. Rev. Lett. 19, 330 (1967).

⁷K. J. Foley, et. al., Phys. Rev. Lett. 11, 425 (1963).

⁸J. Whitmore, et. al., NAL preprint NAL-Pub. 73/25-EXP-7200.141.

⁹10 GeV/c π^-p , P. Fleury, et.al., Proceedings of the 1962 International Conference on High Energy Physics at CERN, P.597.

16 GeV/c π^-p , R. Honecker, et.al., Nucl. Phys. B13, 571 (1969).

25 GeV/c π^-p , A. Erwin, private communication.

50 GeV/c π^-p , V. V. Ammosov, et. al., CERN/D, Ph II/Phys. 73-5 (1973), 50 and 69 GeV/c pp , V. V. Ammosov, et. al., Phys. Lett. 42B, 519 (1972).

12.88 and 28.5 GeV/c pp , B. Y. Oh and G. A. Smith, Michigan State University, private communication.

102 GeV/c pp , J. W. Chapman, et. al., Phys. Rev. Lett. 29, 1686 (1973). 205 GeV/c pp , see reference 8. 303 GeV/c pp , F. T. Dao, et.al., NAL preprint NAL-Pub. 73/22-EXP-7200.037.

¹⁰The approach to constancy of $\langle n_{ch} \rangle/D$ with increasing s has been discussed by several authors, including: O. Czyzewski and K. Rybicki,

Cracow INR Report 800/PH (1972); A. Wroblewski, Remarks on Current Models for Charged Multiplicity Distributions, Paper submitted to XVIth International Conference on High-Energy Physics, Batavia, 1972.

Table I. Topological Cross Sections in 205 GeV/c π^-p
Interactions

Number of Prongs	Events Found	Corrected Number ^a	Cross Section (mb) ^b
0	1	$1^{+3}_{-0.5}$	$.007^{+0.022}_{-0.004}$
1	0		
2 Total	562	639 ± 28	4.79 ± 0.22
Elastic		403 ± 37	3.03 ± 0.3
Inelastic		236 ± 41	$1.76 \pm .30$
3	0		
4	443	460 ± 23	3.45 ± 0.18
5	2		
6	486	506 ± 24	3.79 ± 0.18
7	3		
8	530	540 ± 25	4.05 ± 0.19
9	2		
10	449	454 ± 23	3.41 ± 0.18
11	8		
12	293	291 ± 19	2.18 ± 0.14
13	3		
14	175	173 ± 15	1.30 ± 0.11
15	4		
16	76	69 ± 10	0.52 ± 0.07
17	5		
18	42	42 ± 8	0.31 ± 0.06
19	4		
20	15	13 ± 5	0.10 ± 0.04
21	0		
22	7	5 ± 3	0.04 ± 0.02
23	2		
24	2	2 ± 2	0.015 ± 0.015
Total	3114	3195 ± 57	23.96 ± 0.51

^aTotal error is the statistical error combined with the error on the corrections.

^bThe cross section errors also include errors due to the determination of the total pion path length and the hydrogen density.

Table II. Some Moments of the Multiplicity

Distribution. $f_2 = \langle n(n-1) \rangle - \langle n \rangle^2$, $D = \sqrt{\langle n^2 \rangle - \langle n \rangle^2}$

Parameters	205 GeV/c π^-p	205 GeV/c pp^8
$\langle n \rangle$	8.02 ± 0.12	$7.68 \pm .11$
$\langle n(n-1) \rangle$	71.6 ± 1.8	66.6 ± 1.4
f_2	7.24 ± 0.61	7.66 ± 0.49
$\frac{\langle n \rangle}{D}$	2.05 ± 0.05	$1.96 \pm .05$

FIGURE CAPTIONS

Figure 1 (a) π^-p differential elastic scattering cross section at 205 GeV/c. The curve shown is a fit of $d\sigma/dt$ to the form Ae^{bt} for $0.03 < -t < 0.6$ GeV². There are no data below 0.01 GeV² because of unseen protons. For $0.01 < -t < 0.03$ GeV² the dashed point is the observed number of events and the solid point is corrected for loss of steeply dipping protons using the observed distribution of the proton azimuth around the beam direction. (b) π^-p total cross section σ_{tot} as a function of beam momentum. (c) π^-p elastic scattering cross section σ_{el} as a function of beam momentum. For (b) and (c) the data are from reference 6 (x), reference 1 (+), reference 7 (0), reference 2 (Δ), and this experiment (\blacksquare).

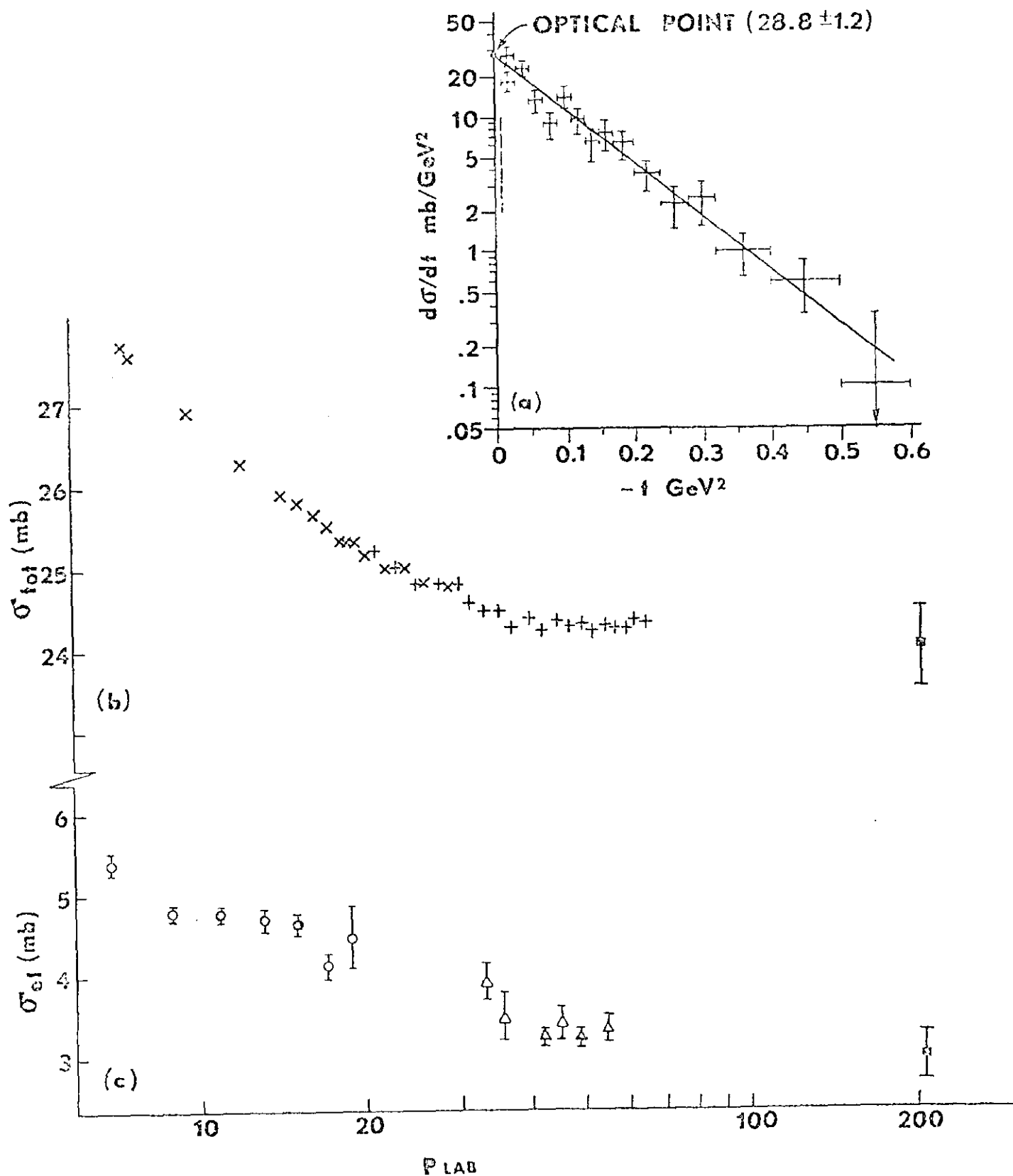


Fig. 1